Geol. Mag. **142** (5), 2005, pp. 617–631. © 2005 Cambridge University Press
doi:10.1017/S0016756805000919 Printed in the United Kingdom

Early Cambrian back-arc volcanism in the western Taurides, Turkey: implications for rifting along the northern Gondwanan margin

S. GÜRSU* & M. C. GÖNCÜOĞLU†

*General Directorate of Mineral Research and Exploration, MAT Department, Ankara, Turkey
†Middle East Technical University, Geological Engineering Department, Ankara, Turkey

(*Received* 22 June 2004; *accepted* 15 February 2005)

Abstract – The Lower Cambrian (Tommotian) Göğebakan Formation in western Central Anatolia is made up of slightly metamorphosed continental to shallow marine clastic rocks with pillowed and massive spilitic lavas and dolerite dykes. Spilitic lavas, commonly amygdaloidal, are albite- and pyroxene-phyric with the metamorphic mineral paragenesis albite + calcite + sericite ± epidote ± tremolite ± chlorite. Dolerite dykes mainly include plagioclase and pyroxene as primary minerals and tremolite ± epidote ± chlorite as low-grade secondary minerals. Geochemical data show that the spilitic lavas and dolerite dykes are sub-alkaline, of oceanic tholeiitic basalt character and display a tholeiitic fractional trend, characterized by an increase in FeO/MgO and Zr and TiO_2 in variation diagrams. They are characterized by relatively high Zr/Y (2–4.5), relatively high Th/Yb (0.15–1.0) and La/Nb (0.5–2.5). Both show marked negative Nb and Ti anomalies relative to Th and La (Ce), implying a subduction-related chemistry. Chondrite-normalized REE patterns display slight enrichment of light REE (spilitic lavas $(La/Yb)_N = 0.79–1.56$; dolerite dykes $(La/Yb)_N = 0.89–3.50$) fairly comparable with MORB. The geochemical similarity of the spilitic lavas and dolerite dykes suggests a co-genetic origin. La/Nb ratios of both types are slightly higher than average MORB values and were possibly formed in the early stages of back-arc basin development. Petrogenetic modelling suggests the mafic rocks of the formation were formed by 9 % batch melting of spinel lherzolite in shallower depths (*c.* 60 km). Taken together the data suggest that the Early Cambrian mafic rocks of the Taurus units were developed in a back-arc basin along the northern edge of Gondwana above the southward-subducting oceanic lithosphere and may represent initial rifting that resulted in separation of the peri-Gondwanan terranes.

Keywords: Western Taurides, Turkey, Early Cambrian, back-arc rifting, Gondwana.

1. Introduction

The Late Proterozoic–Early Palaeozoic interval in northern Gondwana was characterized by a period of extensive igneous activity related to the Cadomian–Late Pan-African orogenic event (e.g. D'Lemos, Strachan & Topley, 1990). These events, initially recognized in SW Europe, are a common feature of numerous terranes which once formed parts of northern Gondwana (e.g. see Murphy, Eguiluz & Zulauf, 2002).

In the Eastern Mediterranean, in Turkey and Iran, the Late Proterozoic–Early Palaeozoic rock units occur in diverse alpine terranes (Fig. 1, Eastern Europe, Turkey and Iran Precambrian rocks) and were identified either as 'Infracambrian sedimentary series' or as orthogneiss inlayers within the metamorphic massifs and attributed to Late Pan-African magmatism (Kozlu & Göncüoğlu, 1997; Göncüoğlu, Dirik & Kozlu, 1997). The relationships and exact ages of sedimentary, mafic and felsic igneous rocks within the alpine metamorphic complexes (Menderes, Central Anatolian and Bitlis metamorphic complexes) are not established and are still a matter of debate (e.g. Erdoğan & Güngör, 2004; Göncüoğlu & Turhan, 1997).

Recently, it has been shown by Gürsu & Göncüoğlu (2001) that the very low-grade metamorphic basement rocks of the Taurides, with Late Neoproterozoic (youngest zircon ages of about 543 ± 7 Ma, Kröner & Şengör, 1990) felsic intrusive rocks, are disconformably overlain by a package of siliciclastic rocks (Göğebakan Formation: Özgül *et al.* 1991) with Early Cambrian (Tommotian: Erdoğan *et al.* 2004) trace fossils. This unit is conformably overlain by Middle Cambrian sediments with a fauna akin to northern Spain (Dean & Özgül, 1994). Within this formation, dykes and mafic volcanic rocks are encountered (Gürsu, Göncüoğlu & Bayhan 2004). Overstep sequences of Early Cambrian magmatism are a common feature of numerous Gondwana-derived terranes, now located within the basement of Variscan and/or Alpine terranes. They were mainly interpreted to reflect rift-related magmatism along the northern margin of Gondwana (e.g. Linnemann *et al.* 2000).

---

† Author for correspondence: mcgoncu@metu.edu.tr

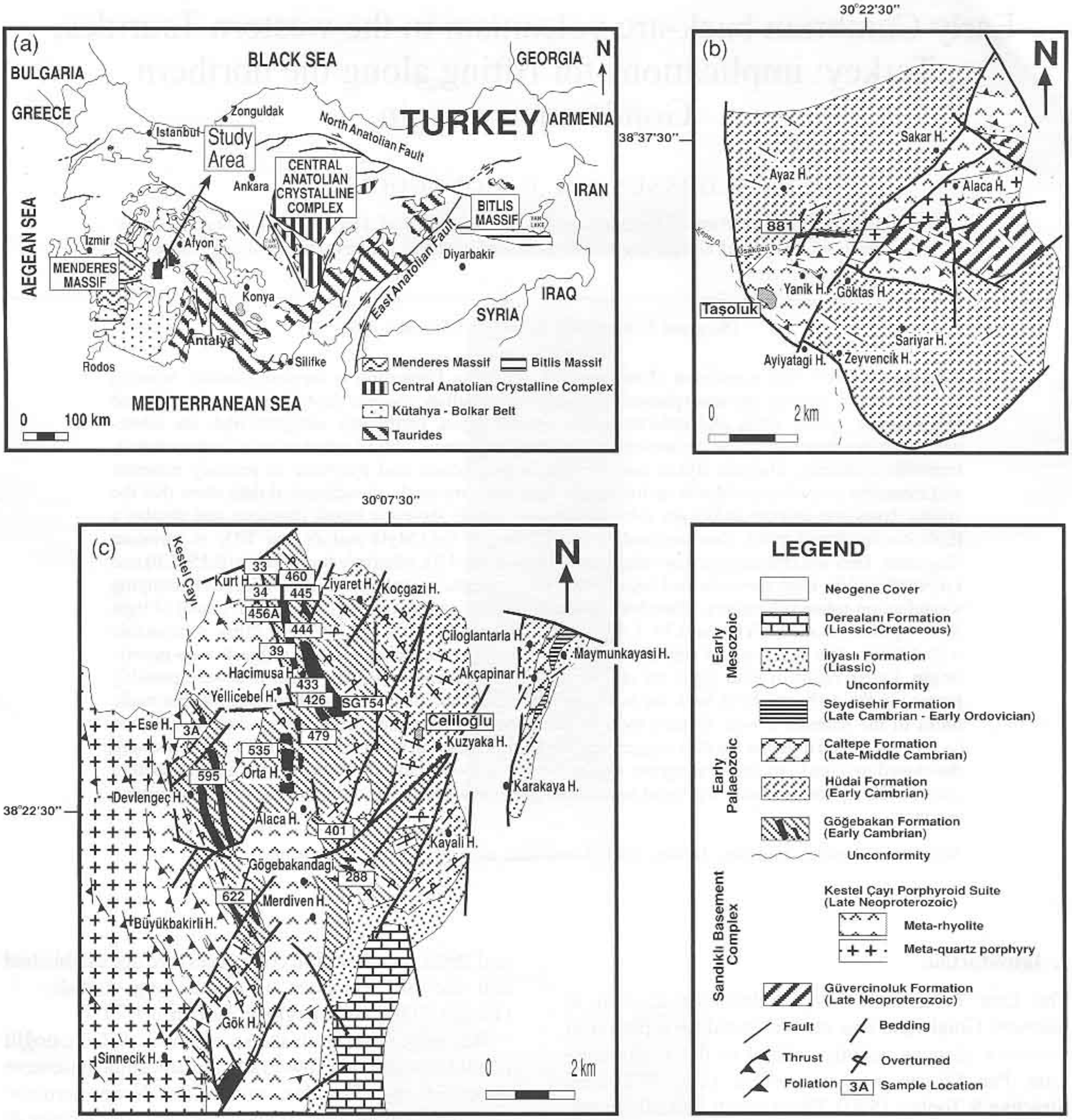

Figure 1. (a) Map showing the location of the study area and the main tectonic units of the Tauride–Anatolide Belt (modified after Göncüoğlu, Dirik & Kozlu, 1997); (b) geological map of northeast of Taşoluk village (south of Afyon); (c) geological map of southwest of Sandıklı (near Celiloğlu village).

In this paper, we will present the results of field studies, coupled with detailed petrological work on the Early Cambrian mafic igneous rocks. The details of local geology, petrogenetic characteristics of Late Neoproterozoic felsic rocks and their metamorphism are presented elsewhere (Gürsu, Göncüoğlu & Bayhan, 2004; Bozkaya, Gürsu & Göncüoğlu, 2004; Gürsu *et al.* 2004). This paper provides a tectono-magmatic approach to the geodynamic evolution of north Gondwana and assesses the applicability of geodynamic models proposed for the Gondwana-derived southern European terranes (e.g. Neubauer, 2002) to the Turkish terranes as previously suggested by Göncüoğlu (1997).

2. Geological framework

Sandıklı (SW Afyon) region in the western central Taurides is characterized by very weak pre-Alpine and Alpine deformations that allow the Late

Neoproterozoic–Early Palaeozoic geological events to be deciphered.

The lowermost rock units in this area constitute the 'Sandıklı Basement Complex' (SBC) (Fig. 1), which includes sub-greenschist sedimentary rocks (Güvercinoluk Formation), associated with felsic volcanic rocks and cut by quartz-porphyry dykes (Kestel Çayı Porphyroid Suite (KCPS): Gürsu, Göncüoğlu & Bayhan, 2004). The Güvercinoluk Formation is composed of black cherts (phtanite) bearing siltstones, recrystallized cherty dolomite lenses, lithic sandstones, slates, phyllites with bands of stromatolitic and dolomitic limestones. The upper part of the formation consists of interbedded debris-flow conglomerate and meta-siltstone/phyllite. The fine-grained meta-sedimentary rocks display a relatively well-developed foliation in which primary clastic texture is commonly obliterated. Quartz + albite + sericite + graphite ± chlorite metamorphic paragenesis is developed. The Kübler Index (KI) values of the white micas in this formation correspond to high anchimetamorphic–low epimetamorphic conditions (Bozkaya, Gürsu & Göncüoğlu, 2004).

The Kestel Çayı Porphyroid Suite (KCPS) is composed of deformed and highly sheared meta-rhyolites and irregularly distributed meta-quartz porphyry dykes cutting both the meta-sedimentary rocks of the Güvercinoluk Formation and rhyolitic carapace. The Sandıklı Basement Complex is intensively mylonitized and variably foliated (Gürsu, Göncüoğlu & Bayhan, 2004). The meta-quartz porphyry dykes yielded a wide range of single zircon $^{207}Pb/^{206}Pb$ ages, the youngest one being 543 ± 7 Ma (Kröner & Şengör, 1990). Geochemical data indicate that the felsic rocks of the KCPS are sub-alkaline and post-collisional and are indicative of an upper crustal source and the co-genetic nature of both the intrusive and extrusive members (Gürsu, Göncüoğlu & Bayhan, 2004).

The SBC rocks are unconformably overlain by the Early Cambrian Göğebakan Formation, which in turn is conformably overlain by the Hüdai, Middle Cambrian Caltepe and Middle/Late Cambrian–Early Ordovician Seydisehir formations, respectively (Fig. 1). The Göğebakan Formation begins with a basal conglomerate that contains sub-rounded to rounded pebbles (meta-rhyolites, black chert (phtanite), recrystallized limestone and meta-siltstones) of the underlying SBC. It includes lenses of coarse-grained arkosic meta-sandstone. Upwards, the formation is composed of red and violet-coloured fluvial sandstones, overlain by a sequence of interbedded red-violet-pink siltstone and mudstone. Interlayers and discontinuous lenses of dark green pyroclastic rocks, spilitic lavas and dolerite dykes are mainly observed in this middle part of the formation (Gürsu & Göncüoğlu, 2001). The lithofacies of the Göğebakan Formation indicate a low-energy shallow marine environment with continental influx (Kozlu & Göncüoğlu, 1995). At the transitional contact, Erdoğan *et al.* (2004) found Tommotion trace fossils. The Celiloğlu and Örenkaya Quartzite members of the Hüdai Formation are composed of siliciclastic rocks that are interpreted as deltaic and beach sediments (Kozlu & Göncüoğlu, 1995). The upper layers of the conformably overlying carbonate succession are characterized by nodular limestones that contain Middle Cambrian trilobites (Dean & Özgül, 1994) and conodonts (Özgül & Gedik, 1973). Anchi-metamorphic storm-beds with nodular limestone bands, shales and meta-sandstones contain Middle–Upper Cambrian to Ordovician fossils (Seydisehir Formation) and constitute the youngest Palaeozoic unit in the Sandıklı area.

The Late Neoproterozoic Sandıklı Basement Complex and Early Palaeozoic rocks are disconformably overlain by a Mesozoic cover that includes conglomerates, sandstones and siltstones of the Liassic İlyaslı Formation, followed by the Liassic–Cretaceous Derealanı Formation (Özgül *et al.* 1991) (Fig. 1).

3. Petrography of the meta-magmatic rocks of Göğebakan Formation

The meta-magmatic rocks of Göğebakan Formation contain spilitic lavas and dolerite dykes. They crop out southwest of Sandıklı (near Celiloğlu village) and northeast of Taşoluk village (south of Afyon) (Fig. 1). Both spilitic lavas and dolerite dykes of the Göğebakan Formation are affected by low-grade metamorphism and are variably foliated. Petrographically, they are classified as spilite and dolerite.

The spilitic lavas are commonly amygdaloidal, albite- and pyroxene-phyric and display quench-textures such as skeletal plagioclase microlites and pyroxene sheaves (Fig. 2a). They are brownish in hand specimen due to extensive oxidation. Lath-shaped plagioclase is albite in composition and pyroxene has been mainly replaced by tremolite. Titanite and opaque minerals occur as accessory minerals. The mineral paragenesis is albite + calcite + sericite +chlorite ± epidote ± tremolite. Amygdales contain quartz, carbonate and rarely zeolite minerals. The glassy matrix of the rock was totally replaced by chlorite minerals.

The dolerites are blasto-ophitic and mainly include plagioclase and clinopyroxene as primary minerals that subophitically enclose laths of plagioclase (Fig. 2b). They contain tremolite ± epidote ± chlorite mineral paragenesis that is indicative for low-grade metamorphism. Plagioclase laths are of andesine/labradorite composition.

4. Geochemistry and petrology

4.a. Analytical techniques

Twenty-two samples (8 of spilitic lavas, 14 of dolerite dykes) collected from the Göğebakan Formation were

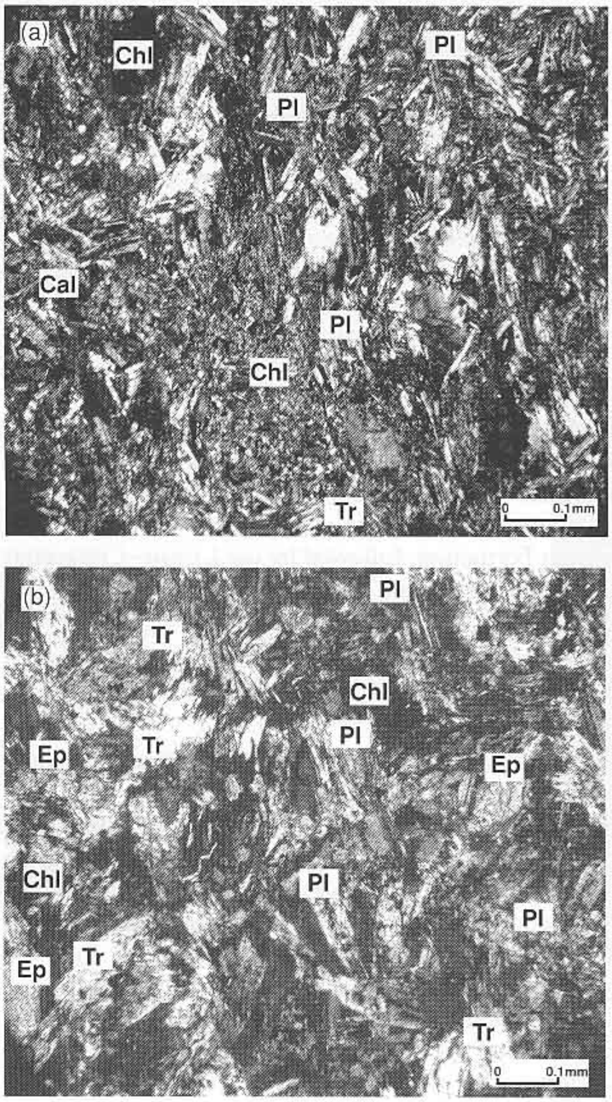

Figure 2. (a) Microphotograph of the spilitic lavas; (b) microphotograph of the dolerite dykes rocks of Göğebakan Formation. Pl – plagioclase, Cal – calcite, Chl – chlorite, Tr – tremolite, Ep – epidote.

analysed for major, trace and rare earth elements (REE) in the ACME Analytical Laboratory (Vancouver, Canada) by using ICP-AES (inductively coupled plasma atomic emission spectrometry) after fusion with $LiBO_2$ and ICP-MS (inductively coupled plasma mass spectrometry) after acid decomposition (HNO_3 of 5 %) (Table 1). Major elements (SiO_2, Al_2O_3, Fe_2O_3, CaO, MgO, Na_2O, K_2O, MnO, TiO_2, P_2O_5 and Cr_2O_3) and Ba, Sc was determined by ICP-AES after fusion with $LiBO_2$. Major element detection limits are about 0.001–0.04 %. The trace elements and rare earth elements (REE) were determined by ICP-MS after acid decomposition (HNO_3 of 5 %). Detection limits of trace and REE elements are 10 ppm for Sc; 5 ppm for V; 2 ppm for Pb; 1 ppm for Ni, W, Sn and Zn; 0.5 ppm for Ba, Co, Ga, Hf, Nb, Rb, Sr, Zr, La and Ce; 0.4 ppm for Nd; 0.1 ppm for Cs, Ta, Th, Tl, U, Y and Sm; 0.05 ppm for Eu, Gd, Dy, Ho, Er, Tm and Yb; 0.01 ppm for Tb and Lu. Analytical precision, as calculated from replicate analyses, is 0.5 % for major elements and varies 0.5–1.5 % for trace and rare earth elements.

4.b. Classification and geochemical variations

The meta-magmatic rocks of the formation are characterized by SiO_2 contents of 45.93–49.56 wt %, MgO of 8.03–12.85 wt % and Fe_2O_3 of 9.24–13.68 wt % in dolerite dykes, whereas spilitic lavas have 45.14–55.38 wt % SiO_2, 1.96–11.62 wt % MgO and 9.03–15.92 wt % Fe_2O_3. To avoid any misinterpretation resulting from post-crystallization chemical changes due to secondary processes, these oxides were checked for possible element mobility by using Zr as discrimination factor. SiO_2–Zr, Al_2O_3–Zr, MgO–Zr, CaO–Zr, Na_2O–Zr and K_2O–Zr pairs are characterized by a lack of linear relationship, whereas Fe_2O_3–Zr, TiO_2–Zr and P_2O_5–Zr diagrams indicate clear positive correlation with Zr for spilitic lavas/dolerite dykes of the formation (Fig. 3). According to Pearce (1983), incompatible LILE (large ion lithophile elements) elements as Cs, Sr, K, Rb and Ba are mobile whereas HFS (high field strength) elements such as REE, Sc, Y, Th, Zr, Hf, Ti, Nb, Ta and P are relatively immobile in low-grade metamorphism. Incompatible elements such as Rb, Sr and Ba elements also display positive relations with K_2O, CaO and $K_2O + Na_2O + CaO$, indicative of alkali mobility during secondary process.

In the Zr/TiO_2 v. Nb/Y diagram of Winchester & Floyd (1977), these mafic rocks plot in the subalkaline basalt field (Fig. 4). Both rock groups also plot in tholeiitic field in the P_2O_5–Zr (Winchester & Floyd, 1977) diagram. The role of the magmatic differentiation that affected the meta-magmatic rocks of the formation is also indicated by the negative trend in the Al_2O_3/TiO_2 v. TiO_2 diagram (Fig. 5).

The magmatic rocks of Göğebakan Formation are characterized by relatively higher Zr/Y (2.30–4.63), slightly lower Zr/Nb (7.3–24.9) and La/Nb (0.43–1.66), higher Th/Ta (2.66–12), Th/Yb (0.25–1.51) and Ta/Yb (0.05–0.38) ratios than the normal mid-ocean ridge basalts (2.64, 31.75, 1.07, 0.75, 0.04, 0.052, respectively: Sun & McDonough, 1989). These features are akin to some subduction-related basalts, back-arc basin basalts and the more enriched type of mid-ocean ridge basalts (Saunders & Tarney, 1984; Sun & McDonough, 1989).

The spider diagram of trace and REE elements is similar to that of oceanic island basalts (OIB) and enriched mid-oceanic ridge basalts (E-MORB) as described by Sun & McDonough (1989). N-MORB normalized (Tarney *et al.* 1981) and chondrite normalized (Sun & McDonough, 1989) spider diagrams of the spilitic lavas and dolerite dykes of the formation reveal a closer correspondence to E-MORB

Table 1. Representative chemical analyses (major, trace, REE) of spilitic lavas and dolerite dykes of Göğebakan Formation

Sample no.	33	34	39	401	456A	479	460	622	881	SGT54	45	79	288	62	Average	152	426	433	444	3A	535	595	445	Average
Rock type	MD	MD	MD	MD	MD	MD	MD	MD	MD	MD	MD	MD	MD	MD	MD	SL	SL	SL	SL	SL	SL	SL	SL	SL
SiO_2	49.56	47.58	45.93	45.79	46.62	46.79	47.2	48.23	47.64	47.01	46.85	47.1	47.69	48.69	**47.33**	50.39	49.29	45.14	52.58	55.36	52.36	46	53.39	**50.56**
Al_2O_3	13.52	14.5	15.25	15.1	15.01	14.95	14.88	16.48	15.15	15.17	14.33	15.98	15.12	15.99	**15.10**	13.1	13.78	17.74	15.02	11.78	15.83	16.66	14.06	**14.74**
Fe_2O_3	10.08	9.94	13.08	13.14	13.07	10.17	13.68	9.68	11.36	10.03	10.14	10.11	9.24	10.23	**10.99**	9.43	15.92	12.66	11.7	13.5	13.94	9.03	14.96	**12.64**
MgO	10.72	11.27	8.03	9.22	8.13	11.99	8.23	9.62	8.75	11.3	12.61	8.62	12.85	9.57	**10.06**	11.62	9.35	10.98	7.5	3.04	5.46	11.53	1.96	**9.12**
CaO	5.62	6.05	8.6	7.3	7.88	6.67	5.34	5.77	8.69	9.22	7.08	10.22	5.22	6.46	**7.15**	5.26	1.06	0.75	1.81	3.31	0.53	3.34	3.47	**2.44**
Na_2O	4.71	4.07	3.77	3.75	3.35	3.75	4.52	4.97	3.95	3.03	2.79	3.19	4.25	2.54	**3.76**	3.78	4.18	5.43	7.06	5.54	6.36	5.25	7.49	**5.63**
K_2O	0.03	0.04	0.09	0.58	0.53	0.37	0.05	0.11	0.17	0.11	1.15	0.94	0.11	2.29	**0.47**	1.14	0.06	0.07	0.04	0.48	0.04	0.02	0.06	**0.24**
TiO_2	0.98	0.97	1.32	1.26	1.27	0.78	1.27	0.61	0.9	0.76	0.89	0.9	0.78	0.74	**0.96**	1.41	1.06	0.83	0.76	0.98	1.36	0.59	0.75	**0.96**
P_2O_5	0.19	0.18	0.13	0.14	0.14	0.09	0.14	0.04	0.07	0.09	0.18	0.11	0.09	0.05	**0.12**	0.16	0.19	0.1	0.04	0.17	0.27	0.05	0.1	**0.135**
MnO	0.24	0.25	0.18	0.35	0.18	0.42	0.19	0.33	0.19	0.23	0.19	0.13	0.39	0.12	**0.24**	0.12	0.18	0.16	0.14	0.13	0.06	0.47	0.17	**0.18**
Cr_2O_3	0.094	0.107	0.029	0.038	0.034	0.09	0.036	0.05	0.033	0.086	0.11	0.128	0.087	0.029	**0.067**	0.054	0.104	0.074	0.09	0.058	0.046	0.06	0.074	**0.07**
LOI	4.1	4.9	3.5	3.5	4.1	4	4.4	4	3.1	2.9	4	3	4.1	3.6	**3.8**	3.9	4.7	6	3.2	5.9	3.7	6.8	3.5	**4.71**
Total	99.88	99.9	99.94	100.24	100.35	100.13	99.96	99.93	100.03	99.98	100.39	100.49	99.97	100.39	**100.11**	100.42	99.91	99.97	99.99	100.28	99.99	99.84	100.02	**100.05**
Ba	98	62	94	438	168	144	44	66	63	51	248	211	59	455	**157.2**	263	216	224	263	143	118	197	110	**191.75**
Sc	36	36	47	45	50	9	46	42	42	40	32	40	38	44	**41.21**	20	37	47	40	24	35	40	45	**36**
Co	49.1	53.2	56	64.4	60.2	48.7	50.7	43.6	45.2	45.9	53.4	49.7	61.3	56.2	**52.68**	52.4	44.7	73.4	52.1	22.8	36	44.7	15.8	**42.73**
Zn	193	239	150	417	132	230	154	612	89	152	145	50	385	47	**213.92**	106	340	138	108	36	151	766	28	**209.12**
Ni	158	219	93	123	96	259	111	158	84	201	225	228	223	114	**163.71**	215	179	227	194	125	117	153	114	**165.5**
Ga	12.3	14.8	21.3	20	21.2	13.4	18.1	14	18.6	15.4	14.8	16.1	14.2	17.7	**13.40**	20.4	14.1	20.5	12	6.7	14.7	13.1	9.6	**13.88**
Hf	2.3	2.4	2.6	2.5	2.8	1.9	2.2	2.1	1.5	1.8	2.1	2	2	1.5	**2.12**	2.7	2.5	2.2	1.6	2.2	2.7	1.2	1.7	**2.1**
Nb	12.3	11.6	5.5	5.1	4.9	3.7	4.3	2.5	2.3	3.1	9.5	7	3.8	1.7	**5.52**	10.5	13.4	4.7	3.3	5	9.2	1.6	3	**6.33**
Rb	0.8	0.9	1.8	16.3	16.3	13.8	1.1	1.7	5.9	3.5	26.4	18.9	2.2	108.8	**15.6**	18.5	1.2	1	<0.5	23.2	1	0.6	1.6	**5.95**
Sr	290	252.4	412.8	214.1	287.3	145.2	84.1	249.6	252.3	336.8	120.2	175.7	152	114.4	**220.49**	213.9	64.4	77.4	80.6	49.8	51.6	144.6	77.1	**94.92**
Ta	0.7	0.6	0.3	0.3	0.3	0.3	<0.1	0.2	0.1	0.2	0.5	0.4	0.2	<0.1	**0.30**	0.6	0.7	0.2	0.2	0.3	0.5	<0.1	0.1	**0.33**
Th	2.3	2.3	0.7	0.5	0.6	0.6	0.4	1.8	0.6	0.8	1.5	2.1	0.5	0.4	**1.07**	2.4	2.3	1.4	0.7	0.8	1.8	0.5	1.2	**1.38**
U	0.4	0.4	0.1	<0.1	<0.1	0.2	<0.1	0.4	0.3	0.2	0.3	0.7	<0.1	<0.1	**0.25**	0.7	1	0.5	<0.1	0.3	2.2	0.2	0.1	**0.63**
V	231	237	365	336	386	226	296	195	269	221	200	246	244	291	**267.3**	167	276	317	76	173	241	192	194	**204.5**
Zr	89.6	86.2	95.4	89.2	91.8	60.2	81.6	71.7	50	54.1	76.6	69.5	64.5	42.7	**73.08**	94.6	98	69.4	57.9	73.4	109.4	39.9	53	**74.45**
Y	25.3	24.9	35.7	31.7	32	16	29.2	20.5	24.7	20.4	23.5	24.4	19.7	21.4	**24.95**	20.4	25.3	25.6	19.9	18.1	23.4	17.3	17.3	**20.91**
La	11.4	12.6	7.9	7.2	6.8	3.5	6.3	6.7	3.5	5.2	11.2	8.7	4.2	2.4	**6.97**	12.7	5.8	6.1	5.5	2.2	6.3	2.3	3.5	**5.55**
Ce	23.7	27	17	15.8	15.9	8.2	14.5	13.7	7.8	11.5	23.4	19.3	9.6	6	**15.24**	26.5	12.3	8.9	10.5	4.3	12.8	5.3	6.3	**10.86**
Pr	3.12	3.37	2.45	2.35	2.3	1.21	2.06	1.71	1.27	1.45	3.01	2.48	1.38	0.99	**2.08**	3.46	2.15	1.37	1.6	0.65	1.65	0.83	0.93	**1.58**
Nd	13.2	13.8	12.4	11	11	5.4	10.6	7.4	7.2	6.8	12.3	10.7	6.1	5.1	**9.5**	15	10.1	7.5	6.4	2.8	6.8	4.3	4.3	**7.15**
Sm	3.3	3.6	3.3	3.3	3.3	1.7	2.8	2	2.3	2	3.1	2.9	2	2.1	**2.69**	4.2	3.4	2.4	1.9	1.2	2.4	1.4	1.3	**2.27**
Eu	1.12	1.28	1.59	1.23	1.24	0.39	1.25	0.71	0.94	0.84	0.94	0.8	0.79	0.84	**1.00**	1.61	1.23	0.93	0.74	0.53	0.85	0.74	0.46	**0.88**
Gd	3.73	3.67	5.23	4.6	4.66	2.22	3.93	2.81	3.14	2.7	3.31	3.55	2.77	2.78	**3.50**	4.58	3.87	3.58	2.67	2.16	3.2	2.12	1.9	**3.01**
Tb	0.63	0.66	0.95	0.87	0.83	0.41	0.73	0.49	0.61	0.5	0.57	0.65	0.51	0.5	**0.63**	0.73	0.69	0.58	0.47	0.42	0.61	0.44	0.41	**0.54**
Dy	4.41	4.3	6.32	5.72	5.98	2.85	4.98	3.53	4.26	3.38	3.94	4.44	3.4	3.58	**4.36**	4.32	4.47	3.83	3.27	2.94	4.02	3.04	2.9	**3.6**
Ho	0.96	0.91	1.3	1.19	1.23	0.62	1.11	0.77	0.94	0.76	0.81	0.85	0.79	0.77	**0.93**	0.77	0.92	0.87	0.72	0.63	0.92	0.63	0.65	**0.76**
Er	2.82	2.84	4.08	3.74	3.7	1.96	3.26	2.44	2.79	2.42	2.59	2.75	2.54	2.53	**2.89**	1.99	2.88	2.81	2.43	2.06	2.87	1.92	2.08	**2.38**
Tm	0.38	0.36	0.52	0.49	0.55	0.27	0.45	0.35	0.38	0.33	0.31	0.35	0.35	0.34	**0.39**	0.26	0.38	0.37	0.31	0.3	0.4	0.28	0.31	**0.32**
Yb	2.53	2.54	3.98	3.49	3.48	1.92	3.01	2.44	2.67	2.26	2.16	2.58	2.43	2.28	**2.69**	1.59	2.48	2.76	2.24	2.03	2.89	1.97	2.03	**2.25**
Lu	0.38	0.41	0.59	0.5	0.54	0.31	0.44	0.35	0.38	0.34	0.37	0.42	0.38	0.34	**0.41**	0.23	0.39	0.44	0.31	0.33	0.49	0.31	0.38	**0.36**
Ti	5874.11	5814.17	7912.07	7552.43	7612.37	4670.31	7612.37	3656.33	5394.59	4555.43	5334.49	5394.59	4675.31	4435.55	**5749.58**	8451.53	6353.63	4975.01	4555.43	5874.11	8151.83	3536.45	4495.49	**5799.18**
Zr/Y	3.54	3.46	2.67	2.81	2.87	3.76	2.79	3.49	2.02	2.65	3.26	2.85	3.27	1.99	**2.95**	4.63	3.87	2.71	2.90	4.05	4.67	2.30	3.06	**3.52**
Zr/Nb	7.28	7.43	17.34	17.49	18.73	16.27	18.97	28.65	21.74	17.45	8.06	9.92	16.97	25.11	**16.52**	9.01	7.31	14.76	17.54	14.68	11.89	24.93	17.66	**14.72**
La/Nb	0.92	1.08	1.43	1.41	1.38	0.94	1.46	2.68	1.52	1.67	1.18	1.24	1.10	1.41	**1.14**	1.21	0.43	1.29	1.66	0.44	0.68	1.43	1.16	**0.87**
Nb/Y	0.48	0.46	0.15	0.16	0.15	0.23	0.14	0.12	0.09	0.15	0.40	0.28	0.19	0.079	**0.22**	0.51	0.53	0.18	0.16	0.27	0.39	0.092	0.17	**0.29**
Th/La	0.20	0.18	0.09	0.07	0.09	0.17	0.063	0.27	0.17	0.15	0.13	0.24	0.12	0.16	**0.16**	0.188	0.39	0.23	0.13	0.36	0.28	0.21	0.34	**0.26**
Th/Ta	3.28	3.83	2.33	1.66	2.00	2.00	4.00	9.00	6.00	4.00	3.00	5.25	2.50	4.00	**3.56**	4.00	3.28	7.00	3.50	2.66	3.60	5.00	12.00	**4.18**
Th/Yb	0.90	0.90	0.17	0.14	0.17	0.31	0.13	0.73	0.22	0.35	0.69	0.81	0.20	0.17	**0.41**	1.51	0.92	0.50	0.31	0.39	0.62	0.25	0.59	**0.61**
Ta/Yb	0.27	0.24	0.07	0.08	0.08	0.15	0.03	0.08	0.03	0.09	0.23	0.155	0.08	0.04	**0.11**	0.38	0.28	0.07	0.08	0.15	0.17	0.05	0.05	**0.15**
Ti/Zr	65.55	67.45	82.93	84.67	82.92	77.58	93.29	50.99	107.89	84.20	69.64	77.62	72.48	103.87	**80.07**	89.34	64.83	71.68	78.67	80.03	74.51	88.63	84.82	**79.06**
$(La/Yb)_N$	3.04	3.35	1.34	1.39	1.32	1.23	1.41	0.71	0.89	1.55	3.50	2.28	1.17	0.71	**1.706**	5.4	1.58	1.49	1.66	0.73	1.47	0.79	1.17	**1.79**

MD – meta-dolerite; SL – spilitic lavas.

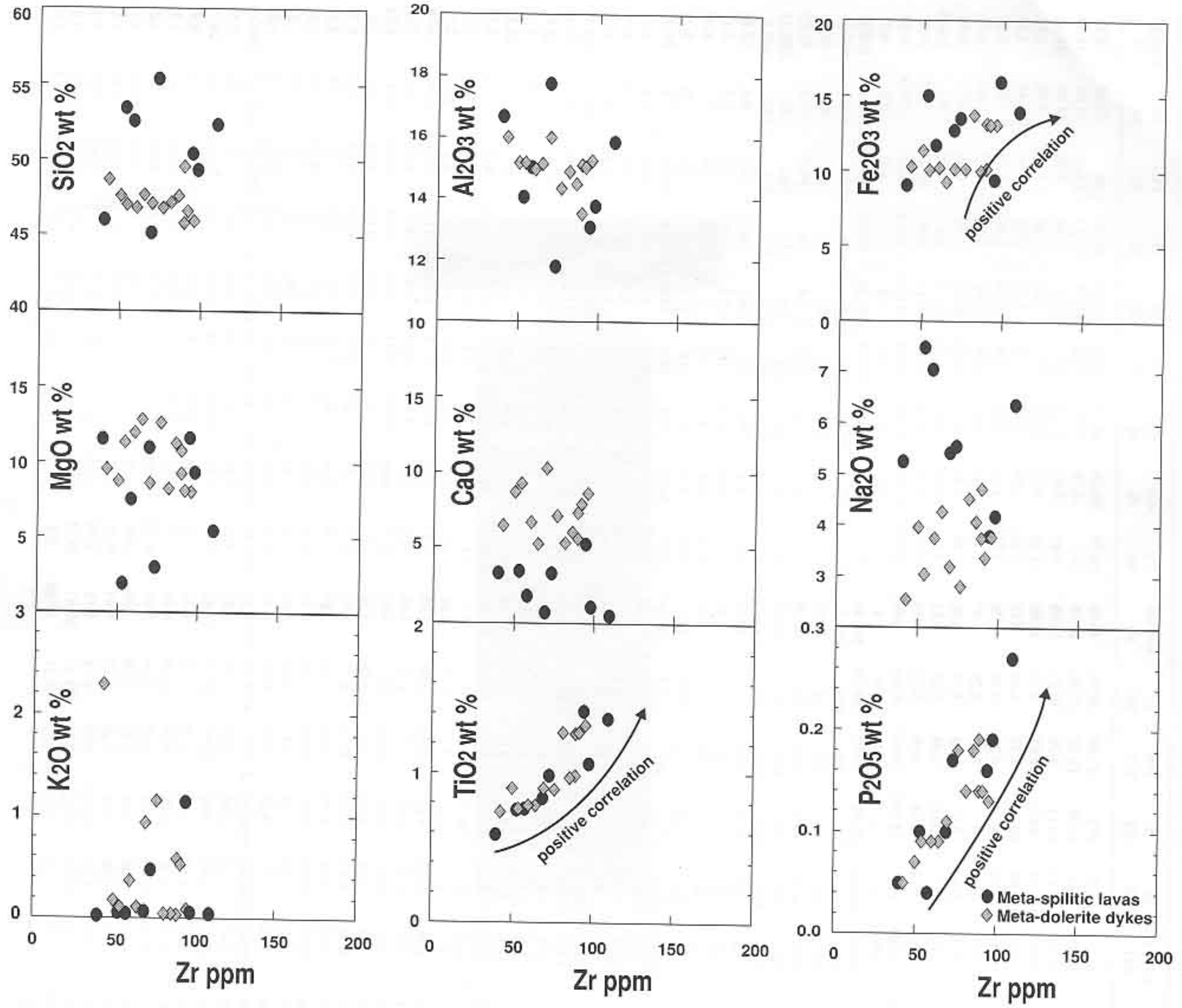

Figure 3. The effects of possible element mobility using Zr as discrimination factor.

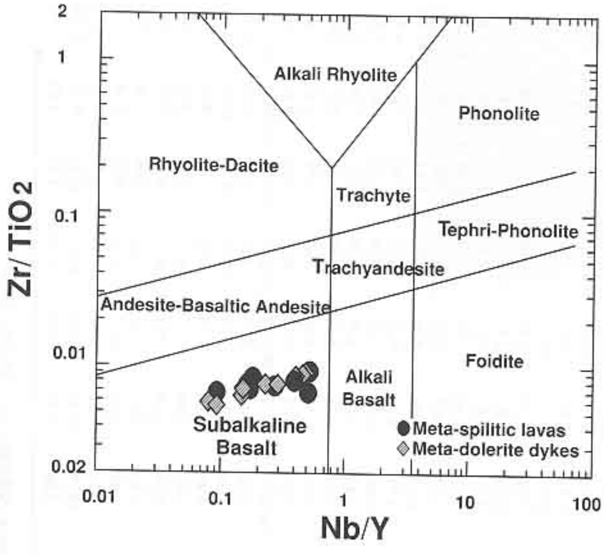

Figure 4. Classification of the mafic rocks of Göğebakan Formation (after Winchester & Floyd, 1977).

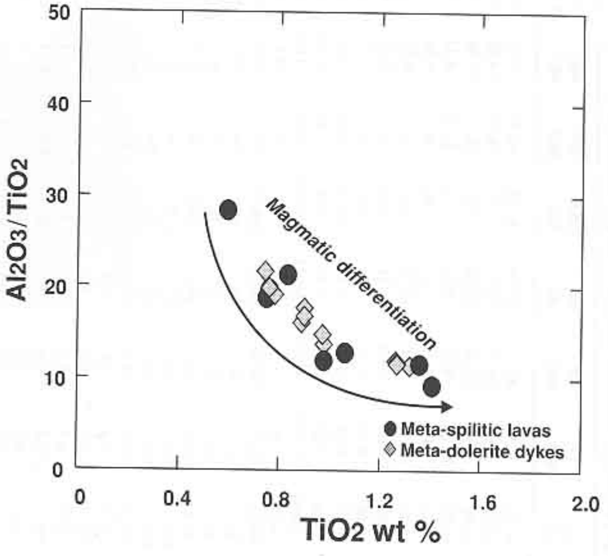

Figure 5. Distribution of the meta-magmatic rocks of Göğebakan Formation on Al_2O_3/TiO_2–TiO_2 variation diagram indicating magmatic differentiation.

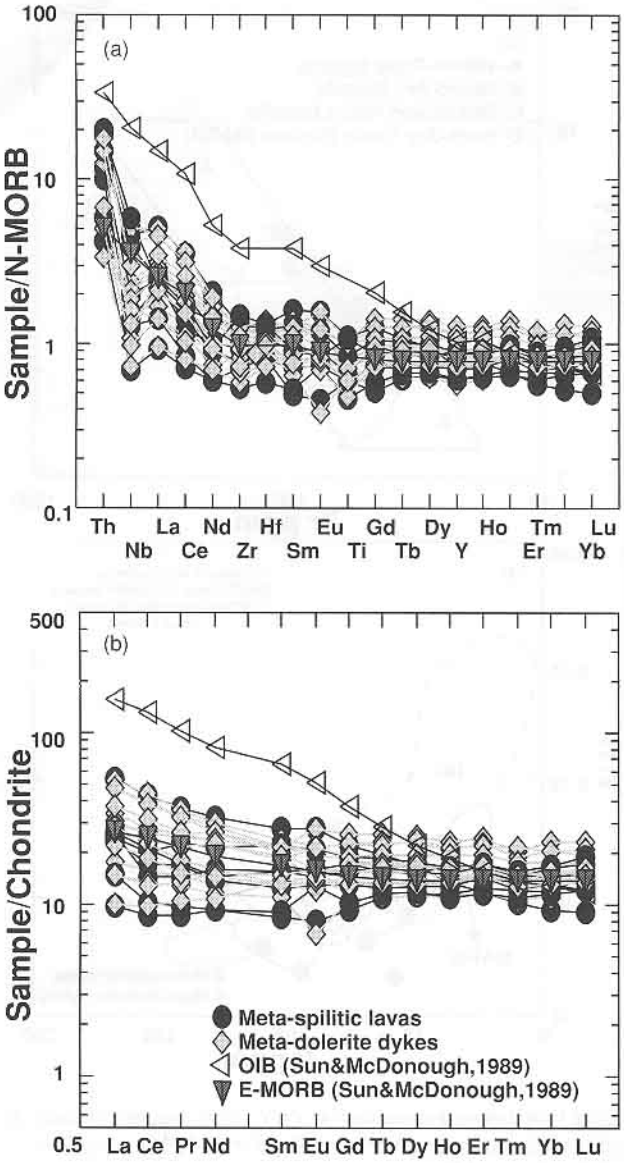

Figure 6. (a) N-MORB normalized multivariation diagram (normalizing values from Sun & McDonough, 1989); (b) chondrite-normalized REE diagram (normalizing values from Sun & McDonough, 1989).

(see Sun & McDonough, 1989) rather than N-MORB and OIB (see Sun & McDonough, 1989) (Fig. 6a, b). They show sharp negative Nb and Ti anomalies relative to Th, La and Ce, implying a subduction-related chemistry and enrichment in LILE (large ion lithophile elements) rather than HFSE (high field strength elements) (Fig. 6a). The absence of a negative Eu anomaly $(\mathrm{Eu/Eu^*})_N$ in spilitic lavas (0.894–1.31) and in dolerite dykes (0.617–1.169) suggests that plagioclase fractionation was not significant (Fig. 6b). Both lithologies are relatively enriched in LREE ($\mathrm{La} = 23 \times$ primitive mantle, $\mathrm{La} = 34 \times$ chondrite; $\mathrm{La} = 23 \times$ primitive mantle, $\mathrm{La} = 35 \times$ chondrite, respectively) and display a horizontal trend by MREE and HREE ($\mathrm{Lu} = 8 \times$ primitive mantle, $\mathrm{Lu} = 15 \times$ chondrite; $\mathrm{Lu} = 7 \times$ primitive mantle, $\mathrm{Lu} = 13 \times$ chondrite, respectively) (Fig. 6b). The $(\mathrm{La/Yb})_N$, $(\mathrm{La/Sm})_N$ and $(\mathrm{Gd/Yb})_N$ ratios, respectively, range from 0.71–3.50, 0.72–2.27, 0.92–1.24 for dolerite dykes and 0.73–5.40, 1.03–1.90, 0.76–2.33 for spilitic lavas. These features resemble the more enriched type of mid-ocean ridge basalts (E-MORB) (1.80, 1.53, 1.02) than N-MORB (0.55, 0.60, 0.98) and OIB (11.58, 2.33, 2.86) (Sun & McDonough, 1989).

The spilitic lavas and dolerite dykes of the formation completely overlap in all diagrams, suggesting a single co-genetic series.

4.c. Tectono-magmatic discrimination

As some oxides (CaO, K_2O and Na_2O) and trace elements (Rb, Sr and Ba) show evidence of mobility during low-grade metamorphism, less mobile high field strength elements were used in tectonic discrimination diagrams. As a whole, spilitic lavas and dolerite dykes are evolved members of a co-genetic tholeiitic suite.

Magmas erupted in subduction-related environments are predominantly enriched in LILE elements (K, Rb, Ba, Th) relative to HFS elements (Nb, Ta, Zr, Hf, Ti). Island arc tholeiites (IAT) have higher LILE/HFS ratios attributed to the subduction influence on back-arc basin basalts (Tarney *et al.* 1981; Pearce, 1983; Saunders & Tarney, 1984; Floyd *et al.* 1991). The analysed samples have subduction-related geochemical features rather than N-type MORB. The spider diagram pattern of trace and REE elements of the studied mafic rocks indicates more Nb and Ti depletion and minor LREE enrichment than HREE (see Fig. 6a, b). LREE enrichment relative to low Nb and Ta contents is generally an indicator of subduction-related composition (Saunders & Tarney, 1984).

Within-plate basalts having higher Ti/Y and higher Nb/Y reflect an enriched mantle source relative to the source of MORB and volcanic arc basalts (Rollinson, 1993). On the Zr/Y–Ti/Y diagrams of Pearce & Gale (1977), the analysed rocks plot in the plate-margin basalts, indicating enrichment in Zr and Ti compared with within-plate basalts (Fig. 7a). Zr/Y plotted against the fractionation index Zr (adapted from Pearce & Norry, 1979) provided an effective discrimination between the basalts from ocean-island arcs, mid-ocean basalts, within-plate basalts and back-arc basin basalts (Rollinson, 1993), and the spilitic lavas and dolerite dykes of the Göğebakan Formation plot in the field of back-arc basin basalts (Fig. 7b).

Back-arc basin basalts (BABB) have notably higher Zr, lower Ti/Zr, V/Ti and Sc/Y values than island arc basalts (IAB) (Woodhead, Eggins & Gamble, 1993). The La/Nb v. Y diagram is an indicator diagram that clearly discriminates between MORB types and subduction-related tholeiitic basalts such as

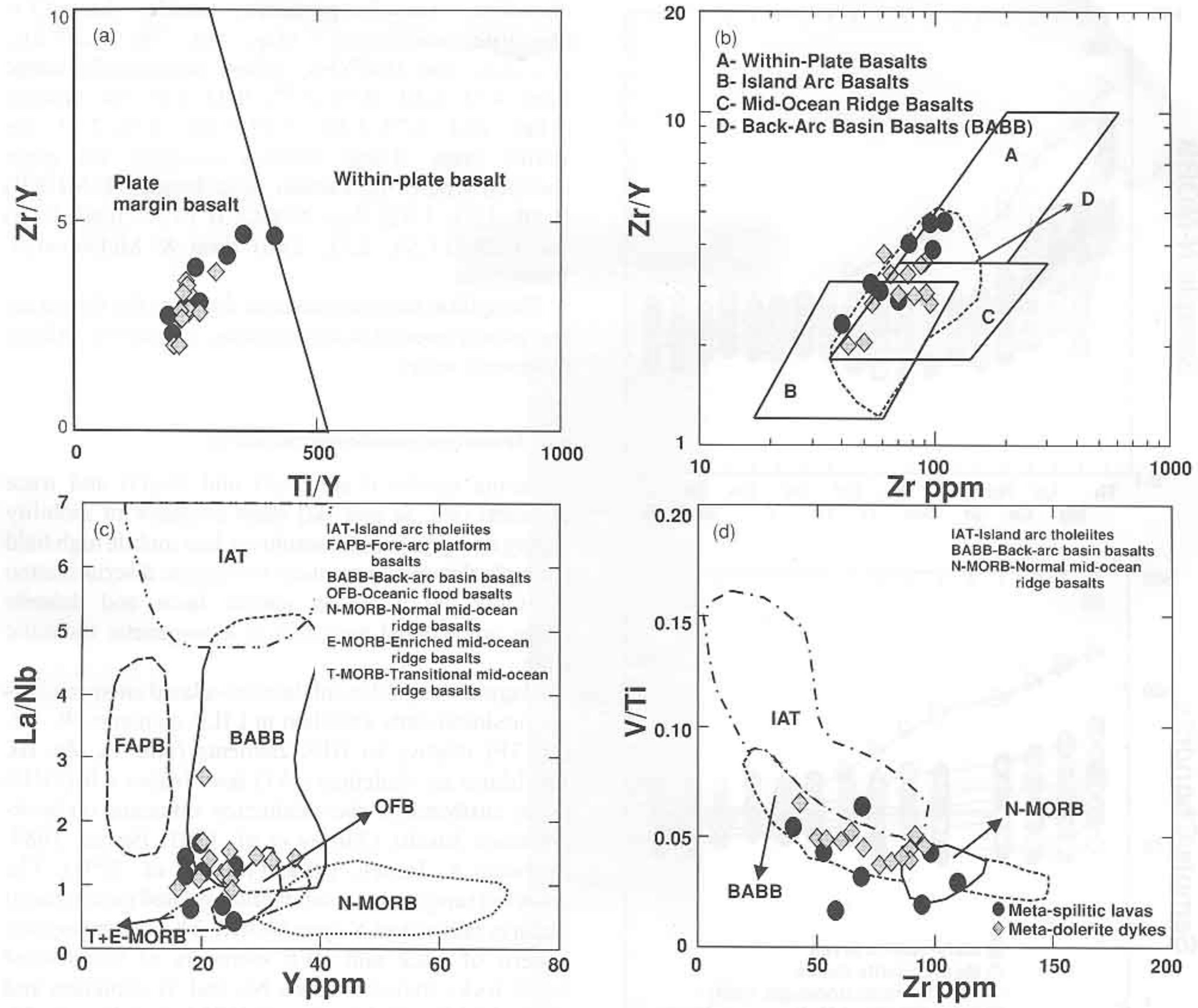

Figure 7. Tectonic discrimination diagrams of meta-magmatic rocks of Göğebakan Formation (a) Zr/Y–Ti/Y diagram (Pearce & Gale, 1977); (b) Zr/Y–Zr diagram (Pearce & Norry, 1979; back-arc basin basalts discrimination from Floyd *et al.* 1991); (c) La/Nb–Y diagram (Floyd *et al.* 1991); (d) V/Ti–Zr diagram (Woodhead, Eggins & Gamble, 1993).

back-arc basin basalts and IAT (Floyd *et al.* 1991). La/Nb ratios are > 5 (commonly > 10) in most arc tholeiites, whereas tholeiites and alkali basalts have ratios between 1 and 5, reflecting the maturity of the arc and the influence of within-plate mantle sources (Brown, Thorpe & Webb, 1984). The low (La/Nb)/Y ratios of both mafic rock-types from the studied area are typical of back-arc basin basalts rather than IAT (Fig. 7c). The spilitic lavas and dolerite dykes of the Göğebakan Formation have lower V/Ti ratios (0.017–0.064 in spilitic lavas, 0.038–0.065 in dolerite dykes) than island arc tholeiites (IAT) and a slightly lower Zr value than N-MORB in the V/Ti–Zr variation diagram of Woodhead, Eggins & Gamble (1993) where the meta-magmatic rocks clearly plot in the BABB field rather than N-MORB or IAT (Fig. 7d).

As a result, the spilitic lavas and dolerite dykes of the Göğebakan Formation may have been erupted in a back-arc basin environment.

4.d. Petrogenesis

The spilitic lavas and dolerite dykes of the Göğebakan Formation have high Cr (225–875 ppm) and slightly high Ni (84–228 ppm) contents. On Al_2O_3/TiO_2–TiO_2 (adapted from El-Nisr, El-Sayed & Saleh, 2001) and Cr–Y variation diagrams of Floyd *et al.* (1991), they display evidence of significant clinopyroxene and plagioclase fractional crystallization (see Figs 6a, 8a).

The spilitic lavas and dolerite dykes of the Göğebakan Formation could have been produced by 5–20 % partial melting of a spinel lherzolite source (Fig. 8a).

Th/Nb ratios (0.09–0.4) of spilitic lavas and dolerite dykes indicate slight enrichment relative to MORB (0.04–0.07) and OIB (0.08) (Sun & McDonough, 1989). Ti/Y (194–414) is generally lower than N-MORB and OIB (272 and 593, respectively: Sun & McDonough, 1989). On the other hand, the V/Ti–Ti/Zr

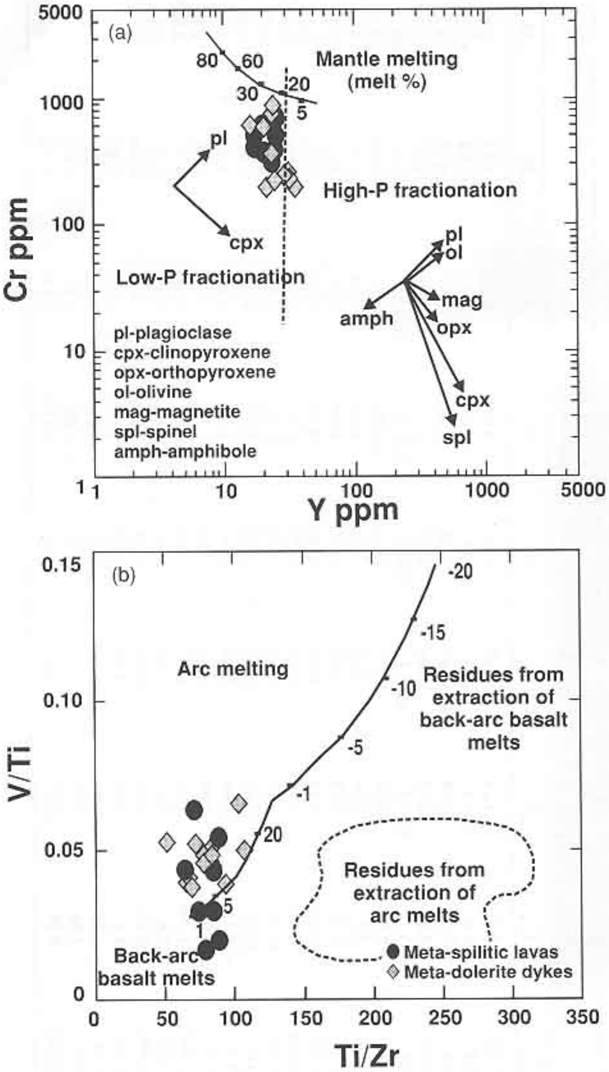

Figure 8. (a) Cr–Y behavior of spilitic lavas and dolerite dykes of Göğebakan Formation with trend of batch melting of a spinel lherzolite source (adapted from Floyd *et al.* 1991). (b) V/Ti–Ti/Zr variations of Woodhead, Eggins & Gamble (1993) displaying model composition of melt and residues formed by 1–20 % melting of a normal mid-ocean ridge basalt source (N-MORB). The diagram also shows an approximate field for residues, formed by extraction of arc melts from N-MORB source.

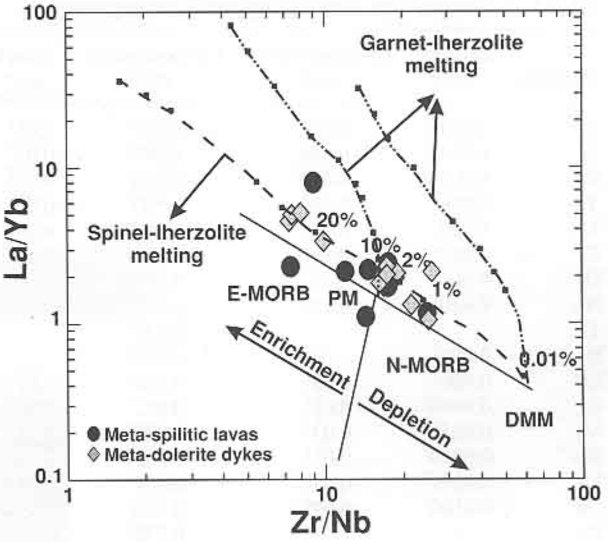

Figure 9. La/Yb–Zr/Nb diagrams (modified after Aldanmaz *et al.* 2000). Spinel lherzolite melting curves indicating $ol^{0.535}$ + $opyr^{0.270}$ + $cpx^{0.170}$ + $sp^{0.030}$ and $ol^{0.600}$ + $opx^{0.280}$ + $cpx^{0.670}$ + $sp^{0.110}$, garnet lherzolite curves indicating $ol^{0.600}$ + $opx^{0.200}$ + $cpx^{0.100}$ + $gt^{0.100}$ and $ol^{0.030}$ + $opx^{0.160}$ + $cpx^{0.880}$ + $gt^{0.090}$, respectively. DMM – depleted mid-ocean ridge basalt mantle, taken from McKenzie & O'Nions (1991, 1995). PM – primitive mantle, N-MORB – normal mid-ocean ridge basalts, E-MORB – enriched mid-ocean ridge basalts are taken from Sun & McDonough (1989).

diagram (see Fig. 8b) suggests that 1 to 20 % melting of N-MORB is required to produce the mafic rocks of the formation.

According to La/Yb–Zr/Nb diagrams, both groups could have formed by 5 to 20 % partial melting of a spinel lherzolite source rather than from a garnet lherzolite source from depleted mid-ocean mantle (DMM) (Fig. 9).

As primitive mantle-normalized trace and REE patterns of mafic rocks were more similar to N-MORB (Saunders & Tarney, 1984) than to OIB (Sun, 1980), spinel lherzolite was used in the modelling studies as the possible source rock (C_0) and partial melting processes were modelled using Rb, Ba, Th, U, Nb, La, Ce, Sr, Nd, Hf, Zr, Sm, Ti, Tb, Y, Sm, Eu, Gd, Er and Lu elements. Proposed source rock is comprised of olivine, orthopyroxene, clinopyroxene and spinel in the relative modal proportions 57:25:16:2 (Woodhead, Eggins & Gamble, 1993). A BABB source is equated with the N-MORB source. For the modelling of batch melting, the formula $C_L/C_0 = 1/(D_0 + F(1 - D_0))$ (Rollinson, 1993) was used, where C_L = the concentration of a trace element in the liquid, C_0 = the concentration of a trace element in N-MORB, D_0 = bulk partition coefficient for a trace element with respect to N-MORB source, F = degree of partial melting (Rollinson, 1993). Mineral/melt partition coefficients for basaltic/basaltic andesite liquids in modelled studies are taken from Arth (1976), Fujimaki, Tatsumoto & Aoki (1984) and Woodhead, Eggins & Gamble (1993) (Table 2). Probable trace element contents were given using 1 %, 1.5 %, 5 %, 8 %, 9 %, 10 % and 15 % partial melting degrees obtained from N-MORB in Table 3. Partial melting (batch melting) of about 9 % of the upper mantle crust data of Sun & McDonough (1989) as source rock seemed to have similarities with observed chemical analyses of both mafic rocks and was correlated respectively with spider diagrams of the studied rocks. N-type MORB and chondrite-normalized trace element and REE patterns suggest that 9 % batch melting of N-MORB seems to fit well to produce both co-genetic spilitic lavas and dolerite dykes of the Göğebakan Formation (Fig. 10a, b). Spider

Table 2. Parameters used in modelling partial melting processes

Elements	Olivine-melt	Orthopyroxene-melt	Clinopyroxene-melt	Spinel-melt
Rb	0.0098[1]	0.022[1]	0.031[2]	0.01[3]
Sr	0.0140[1]	0.040[1]	0.060[2]	0.01[3]
Ba	0.0099[1]	0.013[1]	0.026[2]	0.01[3]
Y	0.010[1]	0.18[1]	0.900[2]	0.01[3]
Ti	0.020[1]	0.10[1]	0.400[2]	0.048[3]
Zr	0.012[1]	0.18[1]	0.100[2]	0.05[3]
Hf	0.0013[1]	–	0.263[2]	–
Nb	0.010[1]	0.15[1]	0.005[2]	–
Th	–	–	0.030[2]	–
U	0.002[1]	–	0.040[2]	–
La	0.0067[2]	0.02[1]	0.056[2]	0.01[3]
Ce	0.0060[2]	0.02[1]	0.092[2]	0.08[3]
Nd	0.0059[2]	0.03[1]	0.230[2]	0.01[3]
Sm	0.0070[2]	0.05[1]	0.445[2]	0.05[3]
Eu	0.0074[2]	0.05[1]	0.474[2]	0.03[3]
Gd	0.0100[2]	0.09[1]	0.556[2]	0.01[3]
Tb	–	–	0.570[2]	0.01[3]
Dy	0.0130[2]	0.15[1]	0.582[2]	0.01[3]
Er	0.0256[2]	0.23[1]	0.583[2]	0.01[3]
Yb	0.0491[2]	0.34[1]	0.542[2]	0.02[3]
Lu	0.0454[2]	0.42[1]	0.506[2]	0.01[3]

Distribution coefficients are for basaltic and basaltic andesite liquids. [1]Arth (1976), [2]Fujimaki, Tatsumoto & Aoki (1984), [3]Woodhead, Eggins & Gamble (1993).

diagrams also display negative trends in Nb, Ti and slight enrichment of LREE than MREE and HREE (Fig. 10a, b).

4.e. Comparison with different BABB data and Pan-African units

The trace and REE patterns of the studied rocks were compared with different mafic rocks of Brno and Bohemia massifs in Central Europe where trace and REE geochemical signatures are transitional between oceanic ridge and island arc basalts (Gill, 1976; Saunders & Tarney, 1979, 1984; Dostal, Patočka & Pin, 2001). Many back-arc basalts display enrichment of LILE elements, and basaltic rocks resembling E-MORB do occur in back-arc basins (Saunders & Tarney, 1984). Saunders & Tarney (1984) pointed out that over-generalized comparisons of the geochemistry of the basaltic rocks from back-arc basins with different ages are contentious because of the wide range of compositions and various degrees of fractional crystallization or partial melting. The meta-mafic rocks of the Göğebakan Formation and the other BABB (having relatively high LILE enrichment) have been normalized to a constant Zr to reduce the various degrees of fractional crystallization and partial melting between the BABB with different ages (Fig. 11). Back-arc basalts have the highest LILE/HFS ratios in mature subduction zones and the lowest LILE/HFS ratios in young subduction zones (Saunders & Tarney, 1984). The geochemical behaviour of Late Proterozoic–Early Palaeozoic mafic rocks of the Göğebakan Formation, Bohemia massifs (Finger *et al.* 2000), Brno (Dostal,

Table 3. Data used in the calculation of partial melting (batch melting)

	D_0	C_0	Average MD	Average SL	F (%)									
					1	1.5	2	5	8	9	10	15	20	25
Rb	0.016246	0.5353	15.6	5.95	20.52	17.26	14.9	8.24	5.63	5.1	4.67	3.26	2.51	2.04
Sr	0.02778	18.21	220.49	94.92	485.6	429.8	385.6	238.4	172.5	157.9	145.67	104.9	81.94	67.23
Ba	0.013253	6.049	157.2	191.75	261.6	215.6	183.37	96.64	65.61	59.26	54.04	37.51	28.72	23.27
Y	0.1949	3.94	24.95	20.91	19.41	19.03	18.67	16.75	15.19	14.73	14.3	12.48	11.07	9.945
Ti	0.10136	1085.1	5749.58	5799.18	9833.5	9448.8	9093.1	7417.3	6263.1	5954.3	5674.5	4594.8	3860.3	3328.3
Zr	0.06884	9.714	73.08	74.45	124.3	117.3	111.06	84.18	67.77	63.63	59.98	46.58	38.08	32.2
Hf	0.04949	0.2676	2.12	2.1	4.53	4.19	3.9	2.76	2.13	1.98	1.85	1.39	1.11	0.93
Nb	0.044	0.6175	5.52	6.33	11.53	10.58	9.78	6.72	5.12	4.75	4.42	3.29	2.62	2.18
Th	0.0048	0.0813	1.07	1.38	5.51	4.12	3.29	1.49	0.96	0.86	0.78	0.527	0.39	0.32
U	0.00754	0.0203	0.25	0.63	1.16	0.905	0.741	0.355	0.23	0.21	0.19	0.13	0.098	0.079
La	0.017979	0.6139	6.97	5.55	22.08	18.76	16.32	9.15	5.28	3.71	2.86	2.33	6.36	5.77
Ce	0.02474	1.6011	15.24	10.86	46.41	40.67	36.18	25.67	15.58	14.23	13.09	9.36	7.28	5.96
Nd	0.047863	1.1892	9.5	7.15	20.72	19.13	17.77	12.46	9.58	8.9	8.31	6.23	4.99	4.16
Sm	0.08869	0.3865	2.69	2.27	3.95	3.77	3.61	2.88	2.39	2.26	2.15	1.71	1.42	1.22
Eu	0.093158	0.1456	1.00	0.88	1.424	1.363	1.308	1.05	0.87	0.83	0.79	0.635	0.53	0.455
Gd	0.11736	0.5128	3.50	3.01	4.06	3.92	3.8	3.17	2.72	2.6	2.49	2.05	1.74	1.51
Tb	0.0914	0.094	0.63	0.54	0.935	0.895	0.857	0.687	0.57	0.54	0.516	0.413	0.344	0.295
Dy	0.13823	0.6378	4.36	3.6	4.34	4.22	4.1	3.51	3.08	2.95	2.84	2.38	2.05	1.8
Er	0.165572	0.4167	2.89	2.38	2.39	2.34	2.28	2.01	1.79	1.73	1.67	1.43	1.25	1.11
Yb	0.2001	0.4144	2.69	2.25	1.99	1.95	1.91	1.73	1.57	1.52	1.48	1.29	1.15	1.036
Lu	0.212038	0.0637	0.41	0.36	0.289	0.284	0.28	0.25	0.23	0.22	0.219	0.193	0.172	0.155

MD – meta-dolerite dykes; SL – spilitic lavas; F – degree of partial melting.

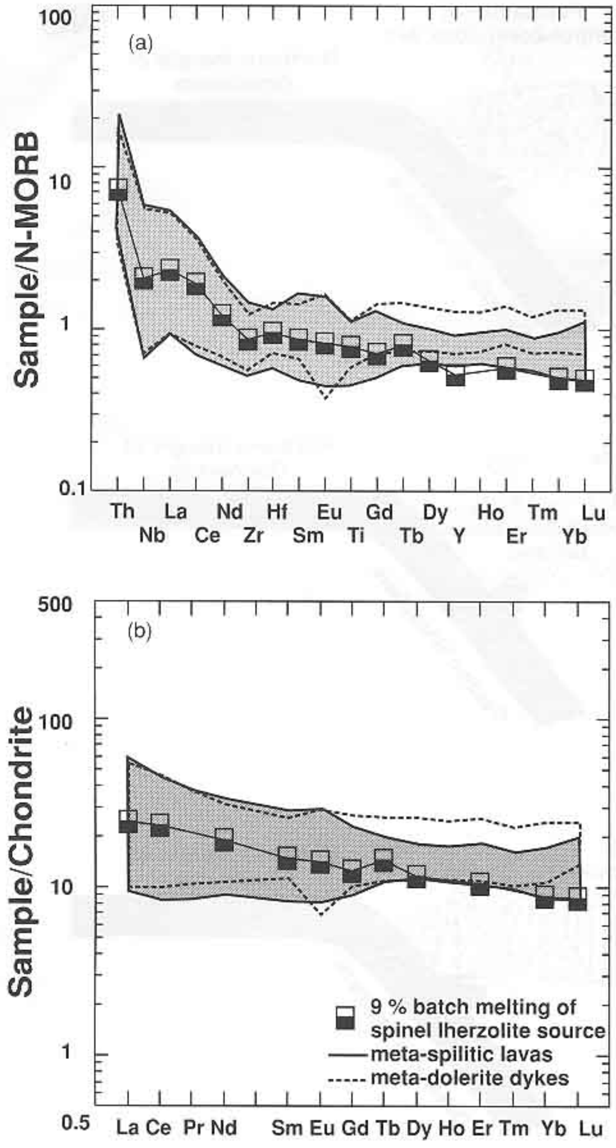

Figure 10. (a, b) Multi-element N-MORB-normalized and REE chondrite-normalized diagrams illustrating 9 % degree of partial melting calculated by non-batch melting of a spinel lherzolite source.

Patočka & Pin, 2001), the Archaean Kaminiskag assemblage (Hollings, Stott & Wyman, 2000) and typical BABB of the Cenozoic Okinawa Trough (Shinjo, 1998) display a roughly concordant spider diagram (Fig. 11) indicating a similar chemical behaviour of these BAB rocks of different ages.

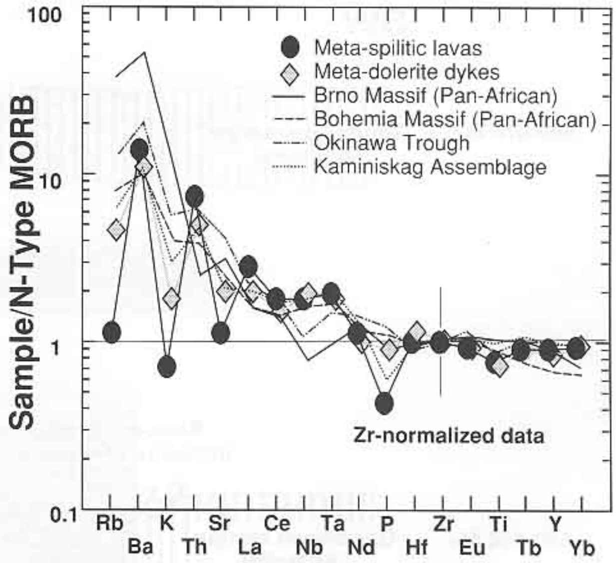

Figure 11. Zr-normalized comperative multi-variation diagram (N-MORB normalizing values from Tarney *et al.* 1981) of back-arc basalts from various basins, adapted from Saunders & Tarney (1979), Kaminiskag Assemblage data from Hollings, Stott & Wyman (2000), Okinawa Trough data from Shinjo (1998) and their correlation with some Late Pan-African meta-basic rocks of Bruno and Bohemian Massifs (Finger *et al.* 2000; Dostal, Patočka & Pin, 2001).

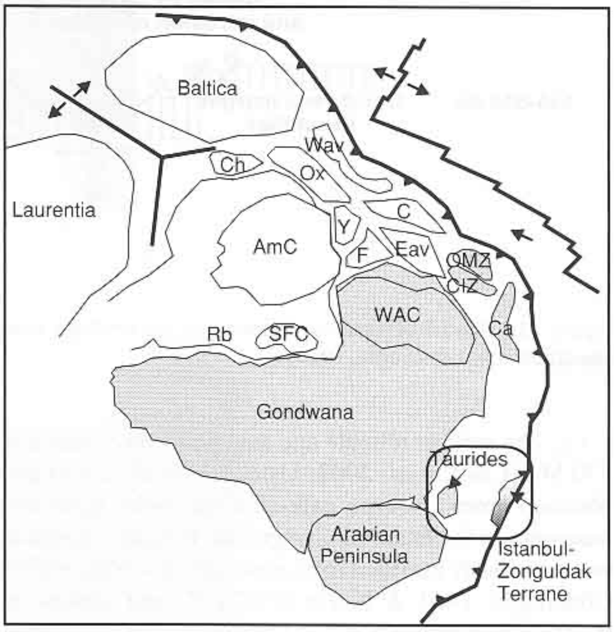

Figure 12. Schematic reconstruction of Late Pan-African (Turkey) during the Cadomian/Pan-African orogeny. AmC – Amazonian craton, C – Carolina, Ca – Cadomia, Ch – Chortis block, CIZ – Central Iberian zone (Iberia), Eav – East Avalonia, F – Florida, OMZ – Ossa-Morena zone (Iberia), Ox – Oaxaquia, Rb – Ribeira, SFC – San Fransisco craton, WAC – West African craton, Wav – West Avalonia, Y – Yucatan (modified after Nance *et al.* 2002; Murphy, Eguiluz & Zulauf, 2002).

5. Discussions on geodynamic implications

The back-arc basin setting of the Early Cambrian Göğebakan Formation meta-magmatic rocks is in good agreement with the geodynamic model proposed by Göncüoğlu & Kozlu (2000) for the Anatolian realm which proposes that the Late Proterozoic–Early Cambrian volcanism in southern Turkey was related to southward subduction of the northern margin of the Gondwana. This model can now be improved by recent geological and geochemical data from the Taurides and northern Anatolia (Fig. 12).

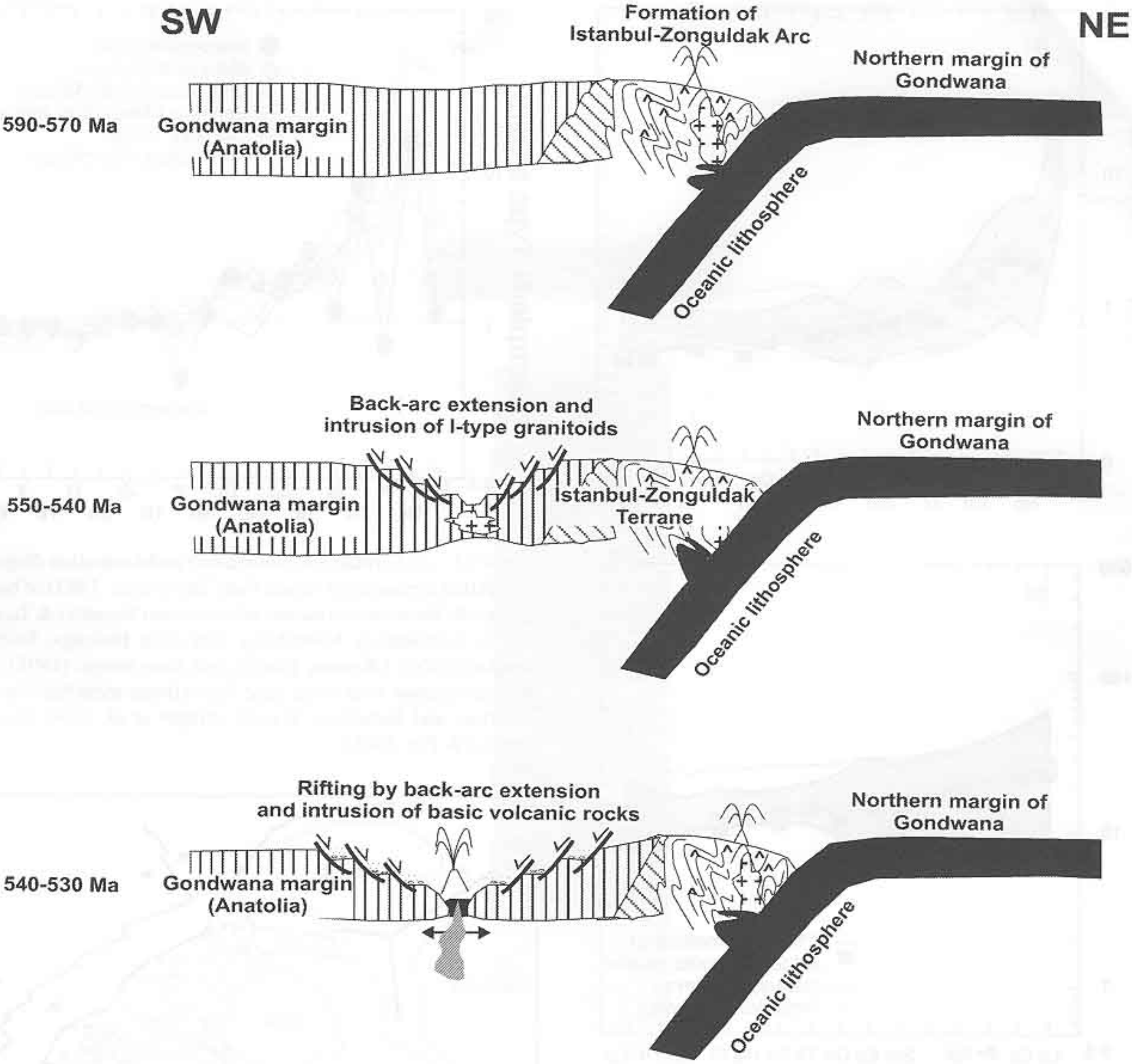

Figure 13. Model of tectonic evolution of the northern margin of Gondwana during Late Neoproterozoic–Early Cambrian time (modified after Göncüoğlu, 1997).

(1) The earliest reliable age data between *c.* 590 and 570 Ma (Chen *et al.* 2002; Ustaömer *et al.* 2003) are obtained from arc-type calk-alkaline rocks from the basement of the Istanbul–Zonguldak Terrane. This unit was previously ascribed to an ensimatic arc complex by Göncüoğlu, Dirik & Kozlu (1997). Recent studies in the Bolu and Armutlu areas (Ustaömer, 1999; Yiğitbaş *et al.* 2004) have shown that these arc-type granitoids intrude an accreted assemblage with supra-subduction-type ophiolites, back-arc-type volcanic rocks and metamorphic rocks of continental crust origin. In our re-evaluation, this assemblage includes arc magmas that intrude the accretionary prism and Precambrian Gondwanan basement and were formed above the southward-subducting northern margin of Gondwana (Fig. 13). This part of the geodynamic model is in good agreement with recent models for Eastern Europe (e.g. Neubauer, 2002) and various Perigondwanan terranes (e.g. Murphy, Eguiluz & Zulauf, 2002; Nance *et al.* 2002) (Fig. 12).

(2) Between *c.* 550 and 540 Ma (Kröner & Şengör, 1990; Loos & Reischmann, 1999), intrusion of mainly I-type granitoids in Menderes Massif and the Taurides occurred. The geochemistry of these granitoids suggests a post-collisional extensional environment (Fig. 13) and may reflect the initial stages of rifting within the Gondwanan continental crust (for a detailed geochemical assessment, see Gürsu, Göncüoğlu & Bayhan, 2004).

(3) The Early Cambrian (*c.* 540–530 Ma) spilitic lavas and dolerite dykes from the Sandıklı area with their typical back-arc geochemical characteristics are interpreted to reflect rifting by back-arc extension where the Gondwanan pericratonic margin had been subject to lithospheric thinning, producing the back-arc basin basaltic rocks (Fig. 13). The formation

of an extensional basin with Early Cambrian siliciclastic successions, tholeiitic volcanism and volcano-sedimentary rocks in the Taurides also correlates with the development in Cadomia and related peri-Gondwanan terranes which are similar in age and tectonic setting (Finger *et al*. 2000; Dostal, Patočka & Pin, 2001; Neubauer, 2002). This rifting episode during the Early Cambrian period very probably resulted in separation of the Istanbul–Zonguldak terrane from the rest of Gondwanan Anatolia and hence the initial opening of a basin to the north of the Taurides. The depositional features of Upper Cambrian to Ordovician successions in the Taurides suggest a shallow platform (e.g. Dean, Uyeno & Rickards, 1999) facing toward a northern oceanic basin, which is a common feature of coeval sediments from Morocco to northern Arabia. On the other hand, the Cadomian basement in the Istanbul–Zonguldak terrane includes arc-type volcanic rocks (e.g. Ustaömer & Rogers, 1999; Yiğitbaş *et al*. 2004), supporting the back-arc setting of the mafic volcanism in the northern Taurides (Figs 12, 13). Moreover, the transgressively overlying Ordovician–Early Silurian rocks are interpreted as graben-facies sediments (Şengör, Yılmaz & Sungurlu, 1984), suggesting the opening of a basin between the Taurides and the Istanbul–Zonguldak terrane (Fig. 13).

6. Conclusions

Summarizing the geological, petrological and geochemical characteristics of slightly metamorphic Early Cambrian spilitic lavas and dolerite dykes from the Sandıklı Area (SW Turkey), the following conclusions are drawn.

(1) The Early Cambrian Göğebakan Formation is composed of continental to shallow-marine clastic rocks alternating with spilitic lavas and pyroclastic rocks, which are cut by doleritic dykes. The succession is very similar to those of the Gondwanan terranes in SW Europe (Finger *et al*. 2000; Dostal, Patočka & Pin, 2001).

(2) Geochemical features of the dolerite dykes and spilitic lavas are indicative of a tholeiitic composition, and overall similarities together with field relationships suggest that they are co-genetic.

(3) Geochemical modelling indicates that these mafic rocks may have been produced by partial melting of an upper mantle source. The mafic magmas were probably derived from the upper mantle (spinel stability field) by 9 % partial melting. REE data indicate that continental contamination was not significant, suggesting the magma passed through a very thin continental crust during back-arc basin spreading. Moreover, the studied rocks show similarities with other BABBs such as those in the Cadomian continental fragments in Europe (Murphy *et al*. 2004).

To conclude, the available geological and geochemical data on the Late Neoproterozoic to Early Palaeozoic igneous events in Turkey indicate that both the Istanbul–Zonguldak and Tauride–Anatolide terranes were dismembered fragments of Gondwanan active margin and located on the eastern continuation of the Eastern European Cadomian and Avalonian terranes.

Acknowledgements. This study was carried out with financial support from the General Directorate of Mineral Research and Exploration (MTA) and State Planning Organization (MTA/DPT Project no. 16AZ). Prof. H. Bayhan (Ankara) is gratefully acknowledged for his contribution. We are grateful to reviewers Prof. Brendan Murphy (Canada) and Prof. Alastair H. F. Robertson (UK) for constructive reading.

References

ALDANMAZ, E., PEARCE, J. A., THIRLWALL, M. F. & MITCHELL, J. G. 2000. Petrogenetic evolution of late Cenozoic, post-collision volcanism in western Anatolia, Turkey. *Journal of Volcanology and Geothermal Research* **102**, 67–95.

ARTH, J. G. 1976. Behaviour of trace elements during magmatic processes – a summary of theoretical models and their applications. *Journal of Research, United States Geological Survey* **4**, 41–7.

BOZKAYA, Ö., GÜRSU, S. & GÖNCÜOĞLU, M. C. 2004. Diagenetic to very low-grade metamorphic evolution of Precambrian–Mesozoic units in the Sandıklı area, Western Taurides, Turkey. In *5th ISEMG* (eds A. A. Chatzipetros and S. B. Pavlides), pp. 1098–1101. 5th International Symposium on Eastern Mediterranean Geology Proceedings, Thessaloniki, Greece.

BROWN, G. C., THORPE, R. S. & WEBB, P. C. 1984. The geochemical characteristics of granitoids in contrasting arcs and comments on magma sources. *Journal of the Geological Society, London* **141**, 413–26.

CHEN, F., SIEBEL, W., SATIR, M. & TERZIOĞLU, M. N. 2002. Geochronology of the Karadere basement (NW Turkey) and implications for the geological evolution of the Istanbul zone. *International Journal of Earth Science* **91**, 469–81.

DEAN, T. W. & ÖZGÜL, N. 1994. Cambrian rocks and faunas, Hüdai area, Taurus Mountains, south-western Turkey. *Bulletin de l'Institut Royal des Sciences Naturelles de Belgique, Sciences de la Terre* **64**, 5–20.

DEAN, W. T., UYENO, T. T. & RICKARDS, R. B. 1999. Ordovician and Silurian stratigraphy and trilobites, Taurus Mountains near Kemer, southwestern Turkey. *Geological Magazine* **136**, 373–93.

D'LEMOS, R. S., STRACHAN, R. A. & TOPLEY, C. G. (eds) 1990. *The Cadomian Orogeny*. Geological Society of London, Special Publication no. **51**, 423 pp.

DOSTAL, J., PATOČKA, F. & PIN, C. 2001. Middle/Late Cambrian intracontinental rifting in the Central West Sudetes, NE Bohemian Massif (Czech Republic): geochemistry and petrogenesis of the bimodal metavolcanic rocks. *Geological Journal* **36**, 1–17.

EL-NISR, S. A., EL-SAYED, M. M. & SALEH, G. M. 2001. Geochemistry and petrogenesis of Pan-African late to post orogenic younger granitoids at Shalatin-Halaib, South Eastern Desert – Egypt. *Journal of African Earth Sciences* **33**, 261–82.

Erdoğan, B. & Güngör, T. 2004. The problem of the core–core boundary of the Menderes Massif and an emplacement mechanism for regionally extensive gneissic granites, Western Anatolia (Turkey). *Turkish Journal of Earth Sciences* **13**, 15–36.

Erdoğan, B., Uchmann, A., Güngör, T. & Özgül, N. 2004. Lithostratigraphy of the Lower Cambrian metaclastics and their age based on trace fossils in the Sandıklı region, southwestern Turkey. *Geobios* **38**, 346–60.

Finger, F., Tichomirowa, M., Pin, C. & Hanžle, P. 2000. Relics of an Early – Panafrican metabasite – metarhyolite formation in the Brno Massif, Moravia, Czech Republic. *International Journal of Earth Sciences – Geologische Rundschau* **89**, 328–35.

Floyd, P. A., Kelling, G., Gökçen, S. L. & Gökçen, N. 1991. Geochemistry and tectonic environment of basaltic rocks from the Misis ophiolitic mélange, south Turkey. *Chemical Geology* **89**, 263–80.

Fujimaki, H., Tatsumoto, M. & Aoki, K. 1984. Partition coefficients of Hf, Zr and REE between phenocrysts and groundmasses. *Journal of Geophysical Research* **89**, 662–72.

Gill, J. B. 1976. Composition and age of Lau Basin and Ridge volcanic rocks: implication for evolution of an inter-arc basin and remnant arc. *Bulletin of the Geological Society of America* **87**, 1384–95.

Göncüoğlu, M. C. 1997. Distribution of Lower Paleozoic rocks in the Alpine terranes of Turkey: Paleogeographic constraints. In *Early Paleozoic Evolution in NW Gondwana* (eds M. C. Göncüoğlu and A. S. Derman), pp. 13–23. Turkish Association of Petroleum Geologists, Special Publication no. 3. Ankara.

Göncüoğlu, M. C. & Turhan, N. 1997. Rock units and metamorphism of the basement and Lower Paleozoic cover of the Bitlis Metamorphic Complex, SE Turkey. In *Lower Paleozoic Evolution in Northwest Gondwana* (eds M. C. Göncüoğlu and A. S. Derman), pp. 75–81. Turkish Association of Petroleum Geologists, Special Publication no. 3. Ankara.

Göncüoğlu, M. C. & Kozlu, H. 2000. Early Palaeozoic evolution of the NW Gondwanaland: data from southern Turkey and surrounding regions. *Gondwana Research* **3**, 315–23.

Göncüoğlu, M. C., Dirik, K. & Kozlu, H. 1997. General characteristics of pre-Alpine and Alpine Terranes in Turkey: Explanatory notes to the terrane map of Turkey. *Annales géologiques des pays helléniques* **37**, 515–36.

Gürsu, S. & Göncüoğlu, M. C. 2001. Characteristic features of the Late Precambrian felsic magmatism in Western Anatolia: implications for the Pan-African evolution in NW PeriGondwana. *Gondwana Research* **4**, 169–70.

Gürsu, S., Göncüoğlu, M. C. & Bayhan, H. 2004. Geology and geochemistry of the pre-Early Cambrian rocks in Sandıklı area: implications for the Pan-African evolution in NW Gondwanaland. *Gondwana Research* 7(4), 923–35.

Gürsu, S., Göncüoğlu, M. C., Turhan, N. & Kozlu, H. 2004. Characteristic features of Precambrian, Paleozoic and Lower Mesozoic successions of two different tectono-stratigraphic units of the Taurides in Afyon area, western Central Turkey. In *5th ISEG* (eds A. A. Chatzipetros and S. B. Pavlides), pp. 80–3. 5th International Symposium on Eastern Mediterranean Geology Proceedings, Thessaloniki, Greece.

Hollings, G., Stott, G. & Wyman, D. 2000. Trace element geochemistry of the Meen-Dempster greenstone belt, Uchi subprovince, Superior Province, Canada: back-arc development on the margins of an Archean protocontinent. *Canadian Journal of Earth Sciences* **37**, 1021–38.

Kozlu, H. & Göncüoğlu, M. C. 1995. Infracambrian Units in Sandıklı area. In *Guide Book to Early Palaeozoic in NW Gondwana* (eds M. C. Göncüoğlu and A. S. Derman), pp. 11–13. Turkish Association Petroleum Geologists, Special Publication no. 2. Ankara.

Kozlu, H. & Göncüoğlu, M. C. 1997. Stratigraphy of the Infracambrian rock-units in the Eastern Taurides and their correlation with similar units in Southern Turkey. In *Early Paleozoic in NW Gondwana* (eds M. C. Göncüoğlu and A. S. Derman), pp. 50–61. Turkish Association Petroleum Geologists, Special Publication no. 3. Ankara.

Kröner, A. & Şengör, A. M. C. 1990. Archean and Proterozoic ancestry in late Precambrian to ealy Paleozoic crustal elements of southern Turkey as revealed by single-zircon dating. *Geology* **18**, 1186–90.

Linnemann, U., Gehmlich, M., Tichomirowa, M., Buschmann, B., Nasdala, L., Jonas, P., Lutzner, H. & Bombach, K. 2000. From Cadomian subduction to Early Palaeozoic rifting: the evolution of Saxo-Thuringia at the margin of Gondwana in the light of single zircon geochronology and basin development (Central European Variscides, Germany). In *Orogenic Processes: Quantification and Modelling in the Variscan Belt* (eds W. Franke, V. Haak, O. Oncken and D. Tanner), pp. 131–53. Geological Society of London, Special Publication no. 179.

Loos, S. & Reischmann, T. 1999. The evolution of the southern Menderes Massif in SW Turkey as revealed by zircon dating. *Journal of Geological Society, London* **156**, 1021–30.

McKenzie, D. P. & O'Nions, R. K. 1991. Partial melt distribution from inversion of rare earth element concentrations. *Journal of Petrology* **32**, 1021–91.

McKenzie, D. P. & O'Nions, R. K. 1995. The source regions of ocean island basalts. *Journal of Petrology* **36**, 133–59.

Murphy, J. B., Eguiluz, L. & Zulauf, G. 2002. Cadomian Orogens, peri-Gondwanan correlatives and Laurentia–Baltica connections. *Tectonophysics* **352**, 1–9.

Murphy, J. B., Pisarevsky, S. A., Nance, R. D. & Keppie, S. A. 2004. Neoproterozoic – Early Paleozoic evalution of peri-Gondwana terranes: Implication for Laurantia – Gondwana connections. *International Journal of Earth Sciences – Geologische Rundschau* **93**, 659–82.

Nance, R. D., Murphy, J. B., Keppie, J. D. & O'Brien, S. J. 2002. A Cordilleran model for the evolution of Avalonia. *Tectonophysics* **352**, 11–31.

Neubauer, F. 2002. Evolution of late Neoproterozoic to Early Paleozoic tectonic elements in central and south-east European mountain belts: review and syntheses. *Tectonophysics* **352**, 87–103.

Özgül N. & Gedik, I. 1973. Orta Toroslarda Alt Paleozoik yasta Caltepe Kirectasi ve Seydisehir Formasyonu'nun stratigrafisi ve konodont faunasi hakkinda yeni bilgiler. *Bulletin of the Geological Society of Turkey* **16**, 39–52.

Özgül, N., Bölükbaşı, S., Alkan, H., Öztaş, Y. & Korucu, M. 1991. Tectonostratigraphic units of the Lake District, Western Taurides, tectonics and hydrocarbon potential of Anatolia and surronding regions. In *Ozan Sungurlu Symposium Proceedings* (ed. S. Turgut), pp. 213–37. Ankara.

PEARCE, J. A. 1983. Role of the sub-continental lithosphere in magma genesis at active continental margins. In *Continental basalts and mantle xenoliths* (eds C. J. Hawkesworth and M. J. Norry), pp. 230–49. Nantwich: Shiva Publications.

PEARCE, J. A. & GALE, G. H. 1977. Identification of ore-deposition environment from trace element geochemistry of associated igneous host rocks. In *Volcanic Processes in Ore Genesis* (ed. M. J. Norry), pp. 14–24. Geological Society of London, Special Publication no. 7.

PEARCE, J. A. & NORRY, M. J. 1979. Petrogenetic implication of Ti, Zr, Y and Nb variations in volcanic rocks. *Contributions to Mineral and Petrology* **69**, 33–47.

ROLLINSON, H. 1993. *Using Geochemical Data: Evaluation, Presentation, Interpretation.* New York: John Wiley & Sons, 352 pp.

SAUNDERS, A. D. & TARNEY, J. 1979. The geochemistry of basalts from a back-arc spreading centre in the East Scotia Sea. *Geochimica et Cosmochimica Acta* **43**, 555–72.

SAUNDERS, A. D. & TARNEY, J. 1984. Geochemical characteristic of basaltic volcanism within back-arc basins. In *Marginal Basin Geology* (eds B. P. Kokelar and M. F. Howells), pp. 59–76. Geological Society of London, Special Publication no. 16.

ŞENGÖR, A. M. C., YILMAZ, Y. & SUNGURLU, O. 1984. Tectonics of the Mediterranean Cimmerides: nature and evolution of the western termination of Palaeo-Tethys. In *The Geological Evolution of the Eastern Mediterranean* (eds J. E. Dixon and A. H. F. Robertson), pp. 77–112. Geological Society of London, Special Publication no. 17.

SHINJO, R. 1998. Petrochemistry and tectonic significance of the emerged late Cenozoic basalts behind the Okinawa Troughs Ryukyu arc system. *Journal of Volcanology and Geothermal Research* **80**, 39–53.

SUN, S. S. 1980. Lead isotopic study of young volcanic rocks from mid-ocean ridges, ocean islands and island arcs. *Philosophical Transactions of The Royal Society, London* **A297**, 409–45.

SUN, S. S. & MCDONOUGH, W. F. 1989. Chemical and isotopic systematics of oceanic basalts: implications for mantle composition and process. In *Magmatism in Ocean Basins* (eds A. D. Saunders and M. J., Norry), pp. 313–45. Geological Society of London, Special Publication no. 42.

TARNEY, J., SAUNDERS, A. D., MATTEY, D. P., WOOD, D. A. & MARSH, N. G. 1981. Geochemical aspects of back-arc spreading in the Scotia Sea and western Pacific. *Philosophical Transactions of the Royal Society, London* **A300**, 263–85.

USTAÖMER, P. A. 1999. Pre-Early Ordovician Cadomian arc-type granitoids, the Bolu massif, West Pontides, northern Turkey: geochemical evidence. *International Journal of Earth Science – Geologische Rundschau* **88**, 2–12.

USTAÖMER, P. A. & ROGERS, G. 1999. The Bolu Massif: remnant of a pre-Early Ordovician active margin in the west Pontides, northern Turkey. *Geological Magazine* **136**, 579–92.

USTAÖMER, P. A., MUNDIL, R., RENNE, P. R. & WHITNEY, D. L. 2003. Time constraints on the tectono-magmatic evolution of the western Pontides (N. Turkey): new U/Pb zircon ages. *European Geophysical Society, Geophysical Research Abstracts* no. 5, 117.

WINCHESTER, A. J. & FLOYD, P. A. 1977. Geochemical discrimination of different magma series and their differentiation products using immobile elements. *Chemical Geology* **20**, 325–43.

WOODHEAD, J., EGGINS, S. & GAMBLE, J. 1993. High field strength and transition element systematics in island arc and back-arc basin basalts: evidence for multi-phase melt extraction and a depleted mantle wedge. *Earth and Planetary Science Letters* **114**, 491–504.

YIĞITBAŞ, E., KERRICH, R., YILMAZ, Y., ELMAS, A. & XIE, Q. 2004. Characteristics and geochemistry of Precambrian ophiolites and related volcanics from the Istanbul–Zonguldak Unit, Northwestern Anatolia, Turkey: following the missing chain of the Precambrian South European suture zone to the east. *Precambrian Research* **132**, 179–206.